PLOS NEGLECTED TROPICAL DISEASES

RESEARCH ARTICLE

Schistosoma mansoni alter transcription of immunomodulatory gene products following *in vivo* praziquantel exposure

Paul McCusker[1,2], **Claudia M. Rohr**[1], **John D. Chan**[1,3,4]*

1 Department of Cell Biology, Neurobiology & Anatomy, Medical College of Wisconsin, Milwaukee, United States of America, **2** Microbe and Pathogen Biology, Institute for Global Food Security, School of Biological Sciences, Queen's University Belfast, Belfast, United Kingdom, **3** Department of Pathobiological Sciences, University of Wisconsin–Madison, Madison, United States of America, **4** Department of Chemistry, University of Wisconsin–Oshkosh, Oshkosh, United States of America

* jchan32@wisc.edu

OPEN ACCESS

Citation: McCusker P, Rohr CM, Chan JD (2021) *Schistosoma mansoni* alter transcription of immunomodulatory gene products following *in vivo* praziquantel exposure. PLoS Negl Trop Dis 15(3): e0009200. https://doi.org/10.1371/journal.pntd.0009200

Editor: Robert M. Greenberg, University of Pennsylvania, UNITED STATES

Received: January 31, 2020

Accepted: February 2, 2021

Published: March 3, 2021

Data Availability Statement: All relevant data are within the manuscript and its Supporting Information files.

Funding: This work was supported by funds from the Therapeutic Accelerator Program and a New Faculty Pilot Grant awarded to J.D.C by the Medical College of Wisconsin; and NIH/NIAID grant 1R21AI153545-01 to J.D.C. The funders had no role in study design, data collection and analysis, decision to publish, or preparation of the manuscript.

Abstract

Control of the neglected tropical disease schistosomiasis relies almost entirely on praziquantel (PZQ) monotherapy. How PZQ clears parasite infections remains poorly understood. Many studies have examined the effects of PZQ on worms cultured *in vitro*, observing outcomes such as muscle contraction. However, conditions worms are exposed to *in vivo* may vary considerably from *in vitro* experiments given the short half-life of PZQ and the importance of host immune system engagement for drug efficacy in animal models. Here, we investigated the effects of *in vivo* PZQ exposure on *Schistosoma mansoni*. Measurement of pro-apoptotic caspase activation revealed that worm death occurs only after parasites shift from the mesenteric vasculature to the liver, peaking 24 hours after drug treatment. This indicates that PZQ is not directly schistocidal, since PZQ's half-life is ~2 hours in humans and ~30 minutes in mice, and focuses attention on parasite interactions with the host immune system following the shift of worms to the liver. RNA-Seq of worms harvested from mouse livers following sub-lethal PZQ treatment revealed drug-evoked changes in the expression of putative immunomodulatory and anticoagulant gene products. Several of these gene products localized to the schistosome esophagus and may be secreted into the host circulation. These include several Kunitz-type protease inhibitors, which are also found in the secretomes of other blood feeding animals. These transcriptional changes may reflect mechanisms of parasite immune-evasion in response to chemotherapy, given the role of complement-mediated attack and the host innate/humoral immune response in parasite elimination. One of these isoforms, SmKI-1, has been shown to exhibit immunomodulatory and anti-coagulant properties. These data provide insight into the effect of *in vivo* PZQ exposure on *S. mansoni*, and the transcriptional response of parasites to the stress of chemotherapy.

Competing interests: The authors have declared that no competing interests exist.

Author summary

The disease schistosomiasis is caused by parasitic worms that live within the circulatory system. While this disease infects over 200 million people worldwide, treatment relies almost entirely on one drug, praziquantel, whose mechanism is poorly understood. In this study, we analyzed the effects of praziquantel treatment on the gene expression of parasites harvested from mice treated with praziquantel chemotherapy. Despite the rapid action of the drug on worms *in vitro*, we found that key outcomes *in vivo* (measurement of cell death and changes in gene expression) occurred relatively late (12+ hours after drug administration). We found that worms increased the expression of immunomodulatory gene products in response to praziquantel, including a Kunitz-type protease inhibitor that localized to the worm esophagus and may be secreted to the external host environment. These are an intriguing class of proteins, because they display anti-coagulant and immunomodulatory properties. Up-regulation of these gene products may reflect a parasite mechanism of immune-evasion in response to chemotherapy. This research provides insight into the mechanism of praziquantel by observing the effect of this drug on worms within the context of the host immune system.

Introduction

The neglected tropical disease schistosomiasis is caused by infection with parasitic *Schistosoma* blood-flukes and afflicts over 200 million people worldwide. These parasites can survive for years–even decades–within the host circulatory system, employing various mechanisms including mimicry of host glycans [1], binding non-immune immunoglobulins [2], and secretion of immunomodulatory extracellular vesicles [3]. With no vaccine available, control of this disease is almost entirely reliant upon chemotherapy with one drug–praziquantel (PZQ)[4].

PZQ's anti-parasitic mechanism of action remains poorly understood. Since the initial studies on this drug over four decades ago, it has been clear that a hallmark of PZQ action on worms is rapid, Ca^{2+}-dependent contractile paralysis [5]. Several targets have since been proposed as the PZQ receptor, including voltage-operated Ca^{2+} channels [6] and a Transient receptor potential channel [7], and a role for PZQ as a Ca^{2+} channel agonist would be in keeping with the obvious, Ca^{2+}-dependent effects of the drug on worm muscle contraction [5]. However, while parasite contraction provides a clear visual readout of drug action *in vitro*, the mechanism of PZQ-evoked parasite elimination *in vivo* is more complex. For example, PZQ causes contractile paralysis of both immature and sexually mature worms *in vitro*, despite the fact that only sexually mature worms and not the immature liver-stage parasites are susceptible to PZQ treatment *in vivo* [8]. Whether PZQ-evoked contraction is related to tegument damage, the other signature effect of anthelmintic exposure, is also unclear. Muscle contraction occurs within seconds, but tegument depolarization occurs over a period of several minutes [9], and pharmacological experiments do not show a correlation between these two phenotypes [10]. Therefore, the *in vitro* phenotype of worm contraction, while useful for drug screening, provides an incomplete readout of PZQ's mechanism of action, which likely encompasses a cascade of events that trigger immune-mediated elimination of the parasites *in vivo*.

PZQ efficacy *in vivo* requires engagement of the host immune system. Following PZQ exposure, sexually mature worms display damage to the tegument surface, which exposes parasite antigens to the host humoral immune system [11] and triggers the recruitment of innate immune cells likely involved in parasite elimination [12]. PZQ is less efficacious at clearing infections from immunocompromised models such as T-cell [13] and B-cell deprived mice

[14]. A requirement for the host immune system may also contribute to PZQ's lack of efficacy against immature parasites, since only after worms become sexually mature and begin egg laying does the host respond with a wave of macrophage recruitment to the liver and an acute Th2 response [15,16]. Notably, PZQ is ineffective against unisex female infections, which do not reach sexual maturity and do not lay eggs [17].

Given the importance of the host immune system to PZQ action, we sought to characterize *Schistosoma mansoni* transcriptional changes following *in vivo* drug exposure. Prior microarray experiments based on expressed sequence tag (EST) libraries have investigated changes in gene expression following *in vitro* PZQ treatment of *S. mansoni* [18] or *in vivo* PZQ treatment of *Schistosoma japonicum* [19]. But no comprehensive study of genome-wide changes in gene expression following *in vivo* PZQ treatment has been performed in the decade since the *S. mansoni* genome has been sequenced. We established conditions for PZQ dosing that elicited a sublethal response in parasites *in vivo*, sequenced the transcriptomes of both sexually mature (7-week-old) and immature (4-week-old) infections treated with either vehicle control or PZQ, and then mapped the expression patterns of differentially expressed transcripts by *in situ* hybridization. These data revealed that numerous up-regulated transcripts were expressed near the esophagus–a location previously identified as a hotspot for expression of immunomodulatory gene products. Specifically, these data highlight a clade of up-regulated Kunitz-type protease inhibitors. Given the immunomodulatory and anti-coagulant activity reported for one of these isoforms, SmKI-1 [20], these changes may reflect the response of parasites to the hostile, immune cell-rich environment of the liver following PZQ treatment.

Materials and methods

Ethics statement

Animal work was carried out with the oversight and approval of the Laboratory Animal Resources facility at the Medical College of Wisconsin, adhering to the humane standards for the health and welfare of animals used for biomedical purposes defined by the Animal Welfare Act and the Health Research Extension Act. Experiments were approved by the Medical College of Wisconsin IACUC committee (approved protocol numbers AUA00006471 and AUA00006735).

In vitro schistosome assays

Female Swiss Webster mice infected with *S. mansoni* cercariae (NMRI strain) were sacrificed by CO_2 euthanasia at 4 weeks (for immature worms) or at 7 weeks post-infection (for mature worms). Immature worms were recovered from mouse livers, and mature worms were recovered from the mesenteric vasculature. Harvested worms were washed in DMEM (ThermoFisher cat. # 11995123) supplemented with HEPES (25mM), 5% v/v heat inactivated FCS (Sigma Aldrich cat. # 12133C) and Penicillin-Streptomycin (100 units/mL). Worms were cultured in 6 well dishes (4–5 mature male worms or 8–10 immature worms in 3mL media per well) at varying concentrations of praziquantel (PZQ, Sigma-Aldrich cat. # P4668) or DMSO vehicle control and imaged to record phenotypes.

Cell proliferation assay

Immature and mature worms (harvested 25 and 49 days post-infection) were treated with drug (37˚C, 14 hours). Worms were washed in drug-free media and allowed to recover for 8 hours, before media was then supplemented with EdU (ThermoFisher Scientific cat. # C10637, 10μM) for a further 14 hours. Worms were fixed in 4% PFA in PBST (PBS + 0.3% triton X-

100), washed in PBST, followed by 1:1 PBST:MeOH, and stored in 100% MeOH at -20˚C. Worms were rehydrated in 1:1 PBST:MeOH, bleached (5% formamide, 0.5X SSC and 1.2% hydrogen peroxide in ddH_2O), rinsed in PBST and permeabilized (0.1% SDS and 0.01mg/ml proteinase K in PBST) for either 30 min (7-week-old schistosomes) or 15 min (4-week-old schistosomes), post-fixed (4% PFA, 10 min), and EdU detection was performed using 1mM $CuSO_4$, 0.1mM Azide-fluor 488 (ThermoFisher Scientific cat. # 760765) and 100mM ascorbic acid in PBS. Worms were stained with DAPI (1μg/ml) and loaded into a 96 well optical bottom black plate for imaging using the ImageXpress Micro Confocal system (Molecular Devices).

In vivo hepatic shift assay

Mice harboring mature infections (6–7 weeks) were administered a fully curative single dose of PZQ (400 mg/kg PZQ dissolved in vegetable oil and delivered by oral gavage) or a sub-curative dose of PZQ (100 mg/kg PZQ solubilized in 50 μL DMSO, then diluted in 200 μL 5% w/v Trappsol (Cyclodextrin Technologies Development cat. # THPB-p-31g) in saline (NaCl 0.9%) solution and delivered by intraperitoneal injection). Mice were sacrificed by CO_2 euthanasia at varying timepoints after drug administration and worms were recovered from either the mesenteries, portal vein or liver. Data = mean ± standard error for 3–5 mice per cohort.

Measurement of caspase 3/7 activation

Pro-apoptotic caspase 3/7 activation was measured in worms harvested from mice following drug treatment using the Caspase-Glo 3/7 Assay Kit (Promega). Worms were harvested from either the mesenteries or liver of mice, then homogenized in assay buffer (PBST, supplemented with HEPES 10mM and protease inhibitor (Roche cOmplete Mini EDTA-free Protease Inhibitor Cocktail)) using a mini mortar and pestle and stored at -80˚C. Worm homogenate (5 pooled male and female worm pairs /125μL assay buffer) was diluted 1:5 in distilled water and added to Caspase-Glo 3/7 substrate (1:1 volume ratio) in solid white 96 well plates. Luminescence was read using a SpectraMax i3x Multi-Mode Microplate Reader (Molecular Devices). Data reflect mean ± standard error of $\geq$ 3 biological replicates.

Transmission electron microscopy

Worms were harvested from infected mice and treated with PZQ as described for movement assays, then fixed overnight at 4˚C in 2.5% glutaraldehyde/2% paraformaldehyde in 0.1M sodium cacodylate (pH 7.3). Worms were then washed in 0.1M sodium cacodylate (3x10 minutes) and post-fixed on ice (2 hours) in reduced 1% osmium tetroxide. Worms were washed in distilled water (2×10 minutes), stained in alcoholic uranyl acetate (overnight, 4˚C), rinsed in distilled water, dehydrated in MeOH (50%, 75% and 95%), followed by successive rinses (10 minutes) in 100% MeOH and acetonitrile. Worms were incubated in a 1:1 mixture of acetonitrile and epoxy resin for 1 hour prior to 2×1-hour incubations in epoxy resin, then cut transversely and embedded overnight in epoxy resin (60˚C). Ultra-thin sections (70nm) were cut onto bare 200-mesh copper grids, stained in aqueous lead citrate (1 minute), then imaged on a Hitachi H-600 electron microscope fitted with a Hamamatsu C4742-95 digital camera operating at an accelerating voltage of 75 kV.

RNA-Seq

For time-course experiments (Fig 1), mice (n = 4 mice per timepoint, across 9 timepoints of 0, 0.25, 1, 3, 6, 9, 12, 24, 49 and 96 hours) were treated with a single, curative dose of PZQ (400 mg/kg) delivered by oral gavage at 7 weeks post-infection, sacrificed by CO_2 euthanasia at the

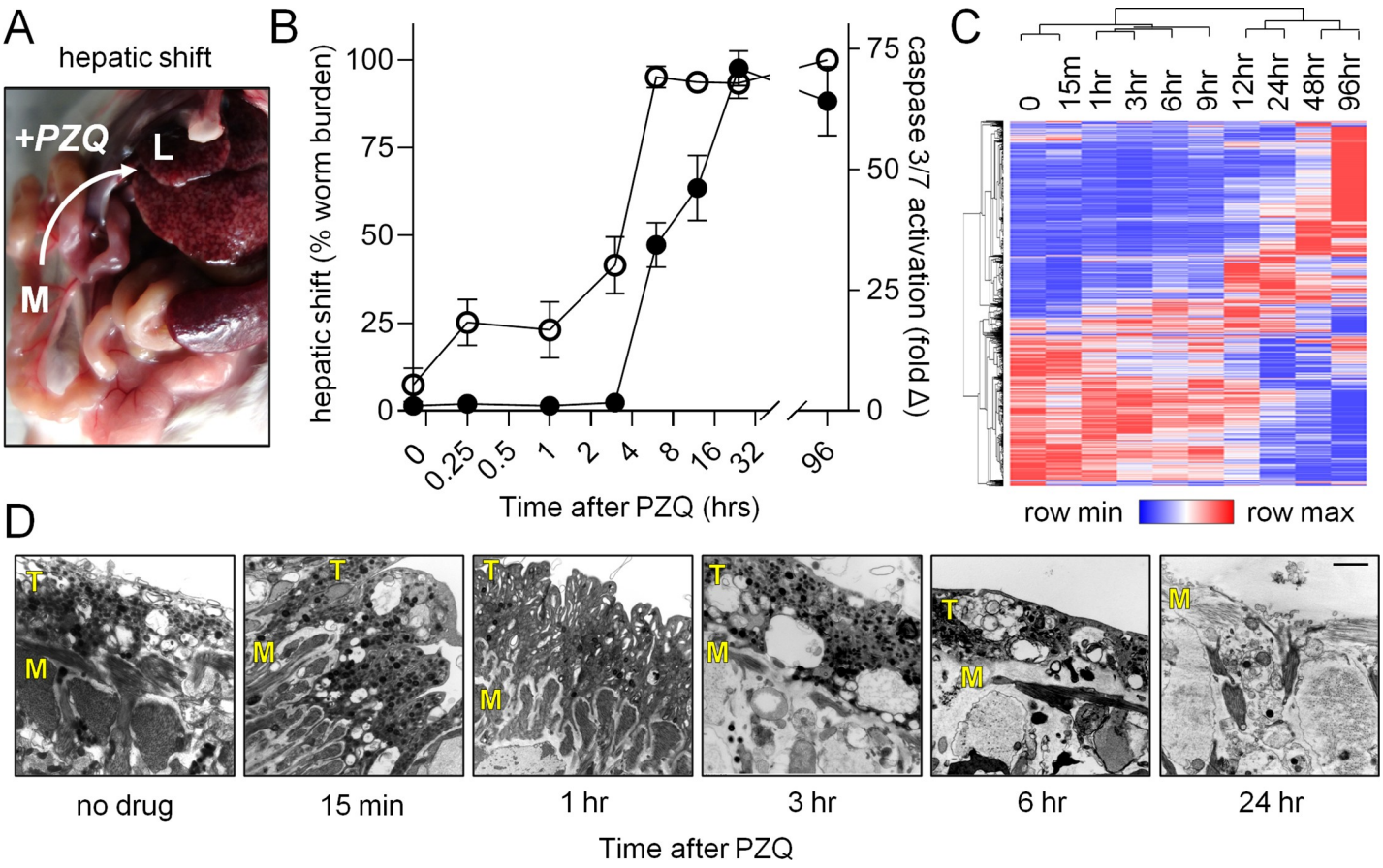

Fig 1. Parasite death occurs following *in vivo* hepatic shift. (A) A curative dose of PZQ (400 mg/kg) was administered to mice 7 weeks post-infection (n = 4 mice per time point) and worms were harvested at various time points from either the mesenteries (M) or the liver (L). **(B)** Time course of parasite hepatic shift (open symbols, left axis) and pro-apoptotic caspase-3/7 activation (solid symbols, right axis). **(C)** Changes in gene expression in worms harvested at various timepoints following PZQ treatment in B. Heatmap reflects minimum (blue) and maximum (red) z-score values for all transcripts showing >1 $\log_2$ fold change and an average TPM > 3 (see S1 File for raw data). **(D)** Transmission electron microscope (TEM) images of the dorsal male body wall showing the time course of tissue damage following *in vivo* PZQ treatment. T = tegument. M = muscle.

https://doi.org/10.1371/journal.pntd.0009200.g001

time-point indicated after drug administration, and adult worms were harvested from the mesenteries or liver. *In vivo*, the adult female schistosome resides within the male gynecophoral canal. Therefore, worms were harvested as male and female pairs and homogenized in Trizol Reagent (Invitrogen), rather than separated. Samples (from n = 4 mice/timepoint) were then pooled to create a single library per timepoint, which was sequenced as outlined below.

For experiments assessing transcriptional changes 14 hours after sub-lethal PZQ treatment, cohorts of n = 5 mice were given vehicle control or PZQ (100 mg/kg) by intraperitoneal injection. This experiment was performed twice, on mice harboring mature worms 7-weeks post-infection (Fig 2) and on mice harboring immature worms 4-weeks post-infection (Fig 3). Animals were sacrificed 14 hours later and worms were harvested. For 4-week-old infections, worms were harvested from the livers of vehicle control and PZQ treated mice. For 7-week-old infections, worms were harvested from either the mesenteric vasculature (vehicle control cohort) or the liver (PZQ treated cohort). Parasites were homogenized in Trizol and stored at -80˚C.

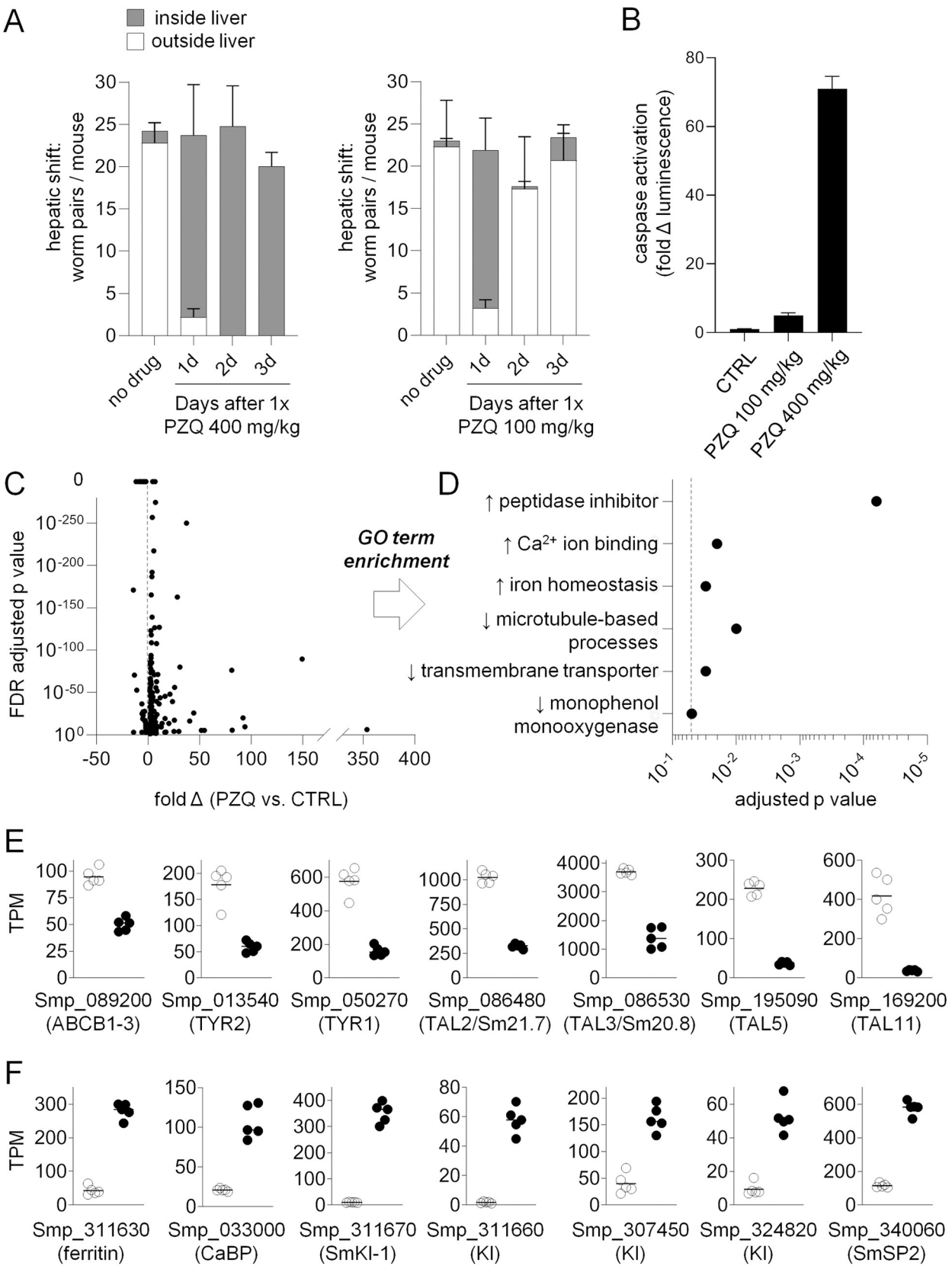
A
inside liver
outside liver
hepatic shift: worm pairs / mouse
no drug
1d
2d
3d
Days after 1x PZQ 400 mg/kg
Days after 1x PZQ 100 mg/kg
B
caspase activation (fold Δ luminescence)
CTRL
PZQ 100 mg/kg
PZQ 400 mg/kg
C
FDR adjusted p value
fold Δ (PZQ vs. CTRL)
GO term enrichment
D
↑ peptidase inhibitor
↑ Ca2+ ion binding
↑ iron homeostasis
↓ microtubule-based processes
↓ transmembrane transporter
↓ monophenol monooxygenase
adjusted p value
E
TPM
Smp_089200 (ABCB1-3)
Smp_013540 (TYR2)
Smp_050270 (TYR1)
Smp_086480 (TAL2/Sm21.7)
Smp_086530 (TAL3/Sm20.8)
Smp_195090 (TAL5)
Smp_169200 (TAL11)
F
TPM
Smp_311630 (ferritin)
Smp_033000 (CaBP)
Smp_311670 (SmKI-1)
Smp_311660 (KI)
Smp_307450 (KI)
Smp_324820 (KI)
Smp_340060 (SmSP2)

Fig 2. Transcriptional response of mature *S. mansoni* to a sublethal dose of praziquantel. (A) Mice were administered PZQ 400 mg/kg or PZQ 100 mg/kg and then euthanized at various time points to count the proportion of parasites found either within the liver (grey stacked bars) or outside the liver (white stacked bars). n = 3–5 mice per time-point. **(B)** Measurement of pro-apoptotic caspase-3/7 activation in homogenate of worms harvested from the livers of mice one day after treatment with PZQ 100 mg/kg or 400 mg/kg. n = 3 mice per time-point. **(C)** Volcano plot of transcripts differentially expressed between worms harvested from mice treated with PZQ (100 mg/kg) or vehicle control. n = 5 mice per cohort. **(D)** Gene-ontology (GO) term enrichment of up-regulated (↑) and down-regulated (↓) lists of transcripts (dashed line, adjusted p value = 0.05). **(E-F)** Examples of differentially expressed gene products containing GO-term annotations in (D). (E) PZQ down-regulated transcripts and (F) PZQ up-regulated transcripts. These data include gene products reported in prior studies (PZQ down-regulation of ABCB1-3 and tyrosinase isoforms, and PZQ up-regulation of ferritin and CaBP isoforms) as well as down-regulated tegument like allergens (TALs) and up-regulated peptidase inhibitors (Kunitz-type protease inhibitors). Symbols represent TPM (Transcripts Per Million) from parasites harvested from individual mice treated with vehicle control (open symbols) or PZQ (solid symbols). Bar = mean TPM value for each cohort of 5 mice.

https://doi.org/10.1371/journal.pntd.0009200.g002

Libraries were generated using the TruSeq Stranded mRNA kit (Illumina) and sequenced using the Illumina HiSeq 2500 system (high-output mode, 50 bp paired-end reads at 20 million reads per sample). Trimmed reads were mapped to the *Schistosoma mansoni* genome (v7.2) using HISAT2. Differentially expressed gene products between vehicle control and PZQ-treated samples were identified using EdgeR (tagwise dispersion model, FDR adjusted p-value < 0.05). For experiments on sublethal drug treatment (Figs 2 and 3), differentially expressed, up and down-regulated transcripts were ranked by fold change and then functional enrichment analysis was performed using g:Profiler [21] to identify enriched GO-terms and KEGG pathways. Principal component analysis was performed using PCAGO [22], an R-based program using DESeq2-normalized counts from S2 and S3 Files and prcomp to visualize clustering of biological samples.

Read counts and differential expression data are contained in S1–S3 Files. FASTQ files containing RNA-Seq data have been deposited in the NCBI SRA database under accession numbers PRJNA597909 and PRJNA602528.

Molecular cloning

RNA was recovered from control worms, or those treated with sublethal dose of PZQ (100mg/kg), using the Purelink RNA Mini kit (ThermoFisher Scientific), with on-column DNase treatment. cDNA was synthesized using the High-Capacity RNA to cDNA kit (ThermoFisher Scientific). Transcripts were amplified using FastStart Taq DNA Polymerase Kit (Millipore Sigma) using primers (S4 File). Amplicons were ligated into pGEM T-easy vector (Promega) and Sanger sequenced.

In situ hybridization

Forward (control) and reverse (target) RNA probes were synthesized from plasmids amplified via PCR (Advantage HD Polymerase Kit, Takara Bio) using T7 or SP6 RNA Polymerases (ThermoFisher Scientific) along with DIG-UTP-labelling mix (Millipore Sigma). Worms harvested from the mesenteries of untreated mice were used to visualize transcripts Smp_076320, Smp_195070, Smp_200150, Smp_246770, Smp_302320, and Smp_311670. Transcripts Smp_008660, Smp_214060 and Smp_336990 were visualized in worms harvested from livers of mice treated with sublethal dose of PZQ (100mg/kg), due to low levels of expression in untreated worms. *In situ* was performed as per reference [23]. Recovered worms were relaxed in 0.25% tricane (2–3 mins), killed in 0.6M MgCl2, and fixed (4% PFA, overnight at 4˚C). Worms were washed in PBST, 1:1 PBST:MeOH, and stored in 100% MeOH, -20˚C. Worms were rehydrated in 1:1 PBST:MeOH, washed in PBST, washed in 1X SSC (10 min), bleached (5% formamide, 0.5X SSC and 1.2% hydrogen peroxide in ddH2O), permeabilized (0.1% SDS and 0.01mg/ml proteinase K in PBST), post-fixed (4% PFA), washed in 1:1 PBST + prehybridization solution, and then incubated in prehybridization solution (2 hours, 52˚C). Worms were

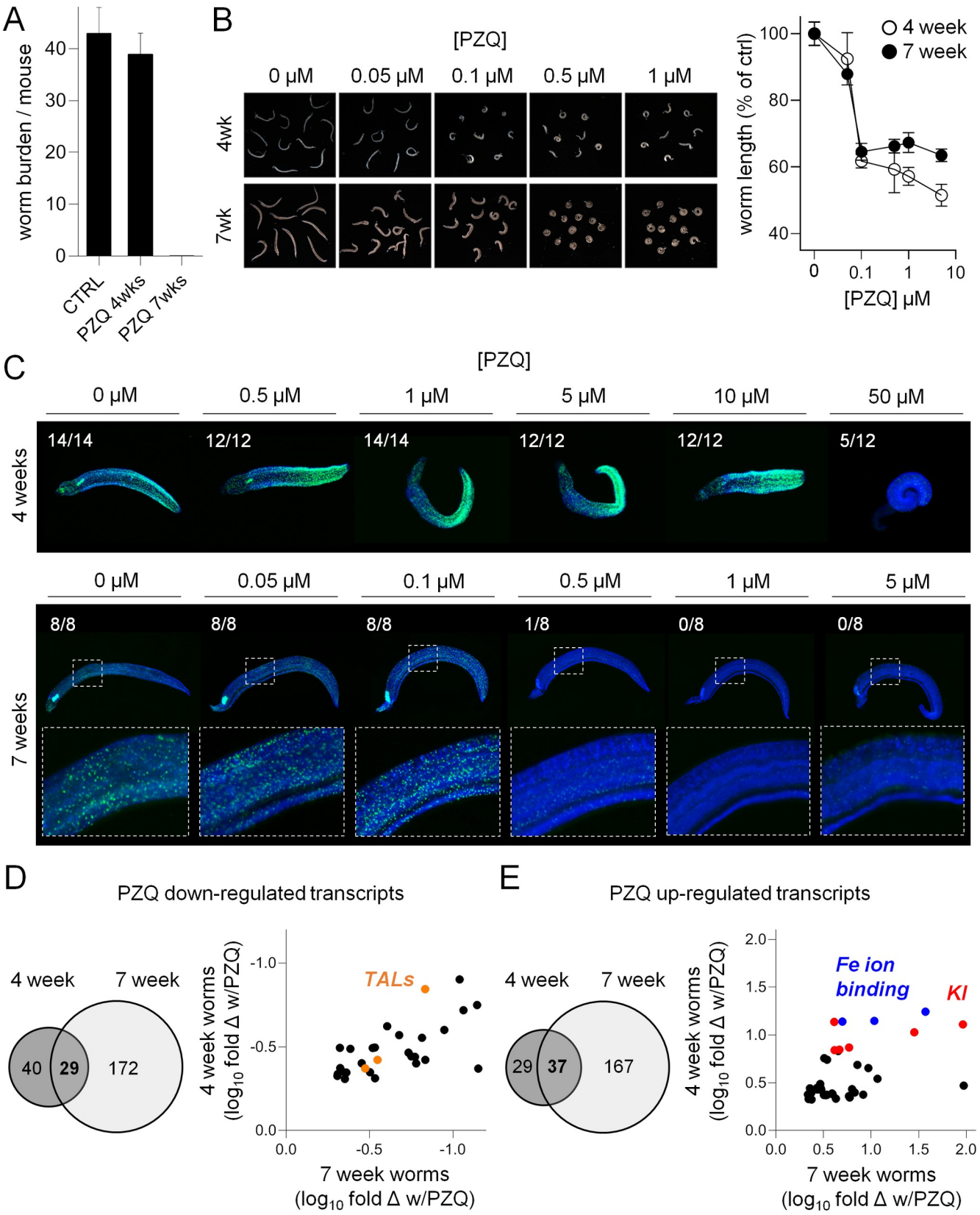
A
worm burden / mouse
40
30
20
10
0
CTRL
PZQ 4wks
PZQ 7wks
B
[PZQ]
0 μM
0.05 μM
0.1 μM
0.5 μM
1 μM
4wk
7wk
4 week
7 week
worm length (% of ctrl)
100
80
60
40
0
0.1
1
10
[PZQ] μM
C
[PZQ]
0 μM
0.5 μM
1 μM
5 μM
10 μM
50 μM
4 weeks
14/14
12/12
14/14
12/12
12/12
5/12
0 μM
0.05 μM
0.1 μM
0.5 μM
1 μM
5 μM
7 weeks
8/8
8/8
8/8
1/8
0/8
0/8
D
PZQ down-regulated transcripts
4 week
7 week
40
29
172
4 week worms
(log10 fold Δ w/PZQ)
-1.0
-0.5
0.0
TALs
7 week worms
(log10 fold Δ w/PZQ)
E
PZQ up-regulated transcripts
4 week
7 week
29
37
167
4 week worms
(log10 fold Δ w/PZQ)
2.0
1.5
1.0
0.5
0.0
Fe ion
binding
KI
7 week worms
(log10 fold Δ w/PZQ)

Fig 3. Praziquantel-evoked transcriptional changes in immature schistosomes. (A) Immature, 4-week-old parasites are unresponsive to PZQ treatment *in vivo*, while 7-week-old infections are cleared. n > 3 mice per treatment. However, **(B)** PZQ has comparable effects on the contraction of both immature and mature worms treated *in vitro*. Left = images of worms treated with varying concentrations of PZQ. Right = quantification of worm body length as a measure of contractile paralysis. **(C)** Effects of *in vitro* PZQ treatment (14 hours) on the mitotic activity of 4-week and 7-week-old worms (worms harvested from mice at 25 and 49 days post-infection, respectively, plus 2 days in culture). Green = EdU incorporation. Blue = DAPI counterstain. Scoring reflects number of EdU positive worms per treatment condition. **(D-E)** Venn diagram of down-regulated and up-regulated transcripts following PZQ treatment of 4-week-old worms relative to vehicle control (n = 5 mice per cohort), and 7-week-old worms (from Fig 2C). Scatter plots reflect $\log_{10}$ fold change of transcripts found in the intersection of both datasets relative to vehicle control. Orange = tegument like allergens (TALs). Red = Kunitz-type protease inhibitors (KI). Blue = Iron ion binding gene products.

https://doi.org/10.1371/journal.pntd.0009200.g003

treated with probes for ≥16 hours at 52˚C, washed in dilutions of SSC (2x and 0.2x) and TNT prior to blocking (1–2 hours in blocking solution of 5% heat-inactivated horse serum (Millipore Sigma), 0.5% Western Blocking Regent (Millipore Sigma), and incubated overnight in anti-DIG-AP (1:2000, Millipore Sigma). Worms were washed (TNTx—0.1 M Tris pH 7.5, 0.15 M NaCl, and 0.1% Tween-20) and incubated in exposure buffer (100mM Tris Base, 100mM NaCl, 50mM MgCl2, 0.1% tween, 4.5μl/ml NBT and 3.5μl/ml BCIP in 10% PVA) until a suitable signal-background ratio was achieved, followed by washing in 100% EtOH (20 minutes).

Quantitative PCR (qPCR)

Worms were harvested from mice 7 weeks post-infection at various timepoints after treatment with a single oral dose of PZQ (400 mg/kg), with three independent biological replicates each consisting of pooled worms collected from 3–4 mice per drug timepoint. Samples were homogenenized in Trizol, and after total RNA-extraction mRNA was purified using the Dynabeads mRNA DIRECT Purification Kit (ThermoFisher Scientific). Samples were then treated with DNase (TURBO DNase, ThermoFisher Scientific), and cDNA was generated using the High Capacity RNA to cDNA kit (ThermoFisher Scientific). qPCRs were run on a BioRad CFX384 or an Applied Biosystems StepOne real-time PCR system using PowerUp SBYR Green Master Mix (Applied Biosystems) and gene specific primers listed in S5 File. Results were analyzed using the delta-delta Ct method to quantify expression relative to glyceraldehyde 3-phosphate dehydrogenase (GAPDH).

Results

Schistosome death occurs after the PZQ-evoked shift from the mesenteries to the liver

Following PZQ exposure, *S. mansoni* shift from the mesenteric vasculature, where mature worms normally reside, to the liver [24–26]. We harvested worms from the mesenteries and livers of mice at various time points after PZQ (400 mg/kg) treatment in order to assess the effects of *in vivo* chemotherapy on parasites (Fig 1A). Worms were processed for measurement of pro-apoptotic caspase 3/7 activation, a readout of worm death, and imaged by transmission electron microcopy, to visualize changes to tissue ultrastructure. Worms displayed activated caspase 3/7 activity beginning 3 hours after PZQ exposure, and this signal reached a maximum at 24 hours after drug treatment. This readout of worm death occurred after the hepatic shift–which began minutes after PZQ administration and was complete within 6 hours (Fig 1B). In parallel to processing these samples, worms were harvested for RNA-Seq at timepoints shown in Fig 1B. A total of 1848 transcripts were evidenced by an average TPM >3 across the timepoints studied and displayed >1 $\log_2$ fold change relative to the controls t = 0 timepoint (S1 File). Hierarchical clustering of these data revealed that the timepoints clustered into two groups, 0–9 hours and 12–96 hours (Fig 1C). The onset of the greatest transcriptional changes,

at around 12 hours after PZQ treatment, corresponds to the period following the parasite hepatic shift.

While changes such as hepatic shift, caspase activation and gene expression took several hours, PZQ caused rapid changes to schistosome tissue ultrastructure. The parasite tegument sits atop layers of body wall muscle, which exhibit a 'bunched' appearance at the earliest timepoint measured after drug administration (15 minutes). However, this effect was not apparent at later timepoints. From 3 hours onward the muscle and tegument displayed a loss of integrity with extensive vacuolization. By 24 hours post drug exposure, the tegument was almost entirely missing in certain regions, exposing underlying layers of body wall muscle (Fig 1D). This time course is notable because PZQ has a relatively short half-life *in vivo*. In humans, PZQ's half-life is approximately 2 hours (reviewed in [27]), and elimination is even more rapid in mice, with a half-life of roughly 30 minutes [28]. This brief window corresponds to the changes in worm musculature observed within an hour after drug treatment, but not the window corresponding to worm death and the most dramatic changes in gene expression. Therefore, these data focused our attention on the events that occur following the parasite hepatic shift, between 12–24 hours after drug exposure.

Establishing sublethal conditions for *in vivo* PZQ treatment

In order to identify an active dose of PZQ for RNA-Seq studies that did not lethally and irreversibly impact schistosomes, we administered various doses of PZQ to mice harboring 7-week-old infections. Prior work has established the range of doses at which PZQ is curative [25,29], and these were used to guide the doses administered in this study. As expected, treatment with a fully curative dose of PZQ (400 mg/kg) caused an irreversible hepatic shift. However, mice treated with low dose PZQ (100 mg/kg) exhibited only a transient parasite hepatic shift (Fig 2A), with worms recovering and returning to the mesenteric vasculature within two days. The sublethal effect of PZQ (100 mg/kg) was verified by measurement of pro-apoptotic caspase activity. Worms harvested from the livers of mice treated with PZQ (400 mg/kg) 14 hours after drug treatment exhibit a 71.0 ± 3.6-fold increase in caspase activation. However, worms harvested from the livers of mice treated with a low dose of PZQ (100mg/kg) at the same timepoint exhibit only a 5.0 ± 0.8-fold increase in caspase activation relative to vehicle controls (Fig 2B). Therefore, low dose PZQ (100 mg/kg) was used for subsequent transcriptomic studies given a sublethal activity on schistosomes.

Transcriptional response of mature parasites to *in vivo* PZQ exposure

Having established a sub-lethal dose of chemotherapy, we analyzed gene expression in 7-week-old parasites harvested from mice 14 hours after treatment with PZQ (100 mg/kg). Equal numbers of male and female worms were harvested from the livers of PZQ treated mice or from the mesenteries of vehicle control treated animals and processed for Illumina sequencing. Reads were mapped to the *S. mansoni* genome (v7) and differential gene expression was assessed between control and PZQ treated samples (S2 File). Up and down-regulated gene products were filtered based on $\geq$2-fold change, FDR adjusted p-value < 0.05, and mean expression level >2 TPM in PZQ treated samples for up-regulated transcripts and mean expression level >2 TPM in control samples for down-regulated transcripts. This revealed 201 transcripts down-regulated and 204 transcripts up-regulated with PZQ treatment (Fig 2C and S2 File).

Broadly, these data confirmed differentially expressed transcripts reported in prior microarray studies (Fig 2D–2F). For example, down-regulated gene products were enriched in gene ontology (GO) terms such as transmembrane transporter activity (ex. ABC transporter

ABCB1-3, Smp_089200, which decreases in *S. mansoni* following PZQ exposure [18,30]) and monooxygenase activity (ex. tyrosinase isoforms required for egg production [31] that are down-regulated in *S. japonicum* following PZQ treatment [19]). Up-regulated transcripts include numerous calcium ion binding proteins, although with smaller predicted molecular weights (~8–10 kDa) than would be expected for calmodulins. These include various 8 kDa Ca^{2+} binding proteins (CaBPs) such as Smp_033000, Smp_032990, and Smp_335140 (the homolog of the PZQ up-regulated *S. japonicum* Contig10880 [19]). Ferritin isoforms (Smp_311630 & Smp_311640) were also up-regulated, as observed in [18,30]). However, the most enriched GO term, 'peptidase inhibitor', was associated with a set of Kunitz-type protease inhibitors (Smp_337730, Smp_311660, Smp_311670, Smp_307450, and Smp_324820) not previously reported in other studies of PZQ response–perhaps because these gene models were recently added in the *S. mansoni* v7 genome.

These transcriptome data also reveal a caveat for utilizing GO term or pathway analysis to study schistosome datasets. These approaches rely on gene annotations mapped from better studied model organisms. However, schistosomes contain many gene products that are unique to flatworms, and either lack annotated protein domains or encode unique proteins that utilize these domains in novel ways. We found that PZQ up and down-regulated gene products were frequently unannotated and more likely to lack GO term annotations, PFAM domains, or have a BLASTp hit in well-studied model organisms (S1 Fig). Many flatworm-specific gene products have not been studied and have unknown expression patterns and function. However, several gene families found within our differentially expressed transcripts have putative roles in parasite development or host-parasite interactions [32–37]. Micro-exon gene (MEG) members are both up-regulated (Smp_336990 (MEG-2.2) and Smp_127990 (MEG-13)) and downregulated (Smp_163710 (MEG-6) and Smp_243770 (MEG-29)). Numerous egg protein CP391S-like transcripts are up-regulated (Smp_194130, Smp_102020, Smp_179970, Smp_201330), as well as several orphan lymphocyte antigen 6 (Ly6) members (transcripts Smp_105220 (SmLy6B), Smp_081900 (SmLy6C), Smp_166340 (SmLy6F), and Smp_345020 (SmLy6J)). Finally, parasite allergens were down-regulated with PZQ treatment, including venom allergen-like (VAL) transcripts (Smp_124060 (SmVAL13) and Smp_154290 (SmVAL27)) and flatworm-specific tegumental allergen-like (TAL) transcripts. These TAL gene products—Smp_086480 (SmTAL2 or Sm21.7), Smp_086530 (SmTAL3 or Sm20.8), Smp_195090 (SmTAL5), and Smp_169200 (SmTAL11)–contain dynein-light-chain domains that account for GO term enrichment related to microtubule-based processes and transport (Fig 2D).

Transcriptional response of immature schistosomes to *in vivo* PZQ exposure

While PZQ cures infections at the sexually mature (7-week-old) parasite stage, the drug is ineffective *in vivo* against immature (4-week-old) infections (Fig 3A, [17]). However, *in vitro* PZQ treatment has similar effects on either 4-week or 7-week old parasites, causing contractile paralysis at approximately equal concentrations (Fig 3B, [8]). Instead, the major difference between these two developmental stages appears to be the effect of PZQ treatment on neoblast-like, mitotically active cells. Immature 4-week-old worms exposed to PZQ for 12 hours, followed by a pulse of EdU, show retained mitotic activity—even after PZQ doses as high as 10 μM. However, similarly treated mature 7-week old worms display a loss of mitotic activity following treatment with concentrations of PZQ ranging from 0.1–0.5 μM (Fig 3C).

Given these data, we were interested to see to what extent the transcriptional response of 4-week-old worms to *in vivo* PZQ exposure resembled that of 7-week-old worms. Mice were

dosed with PZQ (100 mg/kg) or vehicle control 4 weeks post-infection, euthanized 14 hours later, and parasites were harvested from the livers for comparative RNA-Seq just as for 7-week old samples. There were less differentially regulated transcripts in 4-week-old worms relative to the 7-week dataset (69 PZQ down-regulated transcripts and 66 PZQ up-regulated transcripts, S3 File). Of the transcripts differentially expressed in immature worms with PZQ treatment, roughly half were found in the 7-week dataset. GO term enrichment in the 4-week-old worm dataset was broadly similar to the 7-week dataset (S1 Table). PZQ down-regulated gene products in each dataset included various TAL gene products (SmTAL2, SmTAL3 and SmTAL5, Fig 3D), and PZQ up-regulated gene products in both 4 and 7-week old worms included Kunitz-type protease inhibitors and ferritin isoforms (Fig 3E).

Principal component analysis of PZQ treated and control 4 and 7 week old worms showed that the five biological replicates from each experimental cohort clustered together (S2 Fig). The first principal component (accounting for 46.2% of the variance) separated the samples based on developmental stage–drug treated and control worms showed little variation along this axis. Mesentery stage worms differ from liver stage juveniles in that they show more pronounced sexual dimorphism, and unlike young worms they typically live as mated pairs producing eggs. The second principal component (31.41% of variance) differentiated samples based on drug treatment, with samples showing little variation based on developmental stage. The latter is consistent with the shared changes in gene expression observed following PZQ treatment in both of these developmental stages (Fig 3D and 3E).

Tissue localization of transcripts differentially expressed following PZQ exposure

We performed *in situ* hybridization to localize the expression patterns of PZQ up and down-regulated gene products in adult (7-week-old) worms. Many down-regulated transcripts localized to the germ line (Fig 4A)–with expression patterns staining the female vitellaria (Smp_076320 (myb/sant-like) and ovaries (Smp_246770 (cadherin)), as well as the male testes (Smp_195090 (SmTAL5)). This is consistent with PZQ treatment causing loss of mitotic activity in germ line tissues.

Many PZQ up-regulated transcripts, such as Kunitz-type protease inhibitors, heat-shock protein, MEG 2.2, alpha-crystallin and phosphoglycerate kinase displayed expression patterns with varied localization within the male body. However, these commonly displayed strong expression at the anterior of the worm, with staining of glands located around the esophagus (Fig 4B). The schistosome esophagus has been shown to be a secretory organ [38], and various MEG and VAL gene products have been localized to this structure [33].

Time course of PZQ-evoked changes in gene expression

Analysis of differential gene expression was performed on worms harvested at a fixed timepoint (14 hours) after drug exposure. RNA-Seq data from the time-course following administration of single oral dose of PZQ (400 mg/kg) broadly confirmed these changes in gene expression–various Kunitz type protease inhibitors were upregulated while numerous tegument-like allergens (TALs) were down-regulated. However, a limitation of that experiment is that each timepoint consisted of a single sequencing run of pooled biological samples (Fig 1C and S1 File)–therefore, we performed qPCR on new samples harvested across a similar time course to validate these with independent biological replicates (S3 Fig). These qPCR data were consistent with the trends in gene expression observed with RNA-Seq, with changes in gene expression most pronounced between 12–24 hours after drug administration. These timepoints are later than the brief window during which PZQ reaches a C_{max} *in vivo* (Fig 5A,

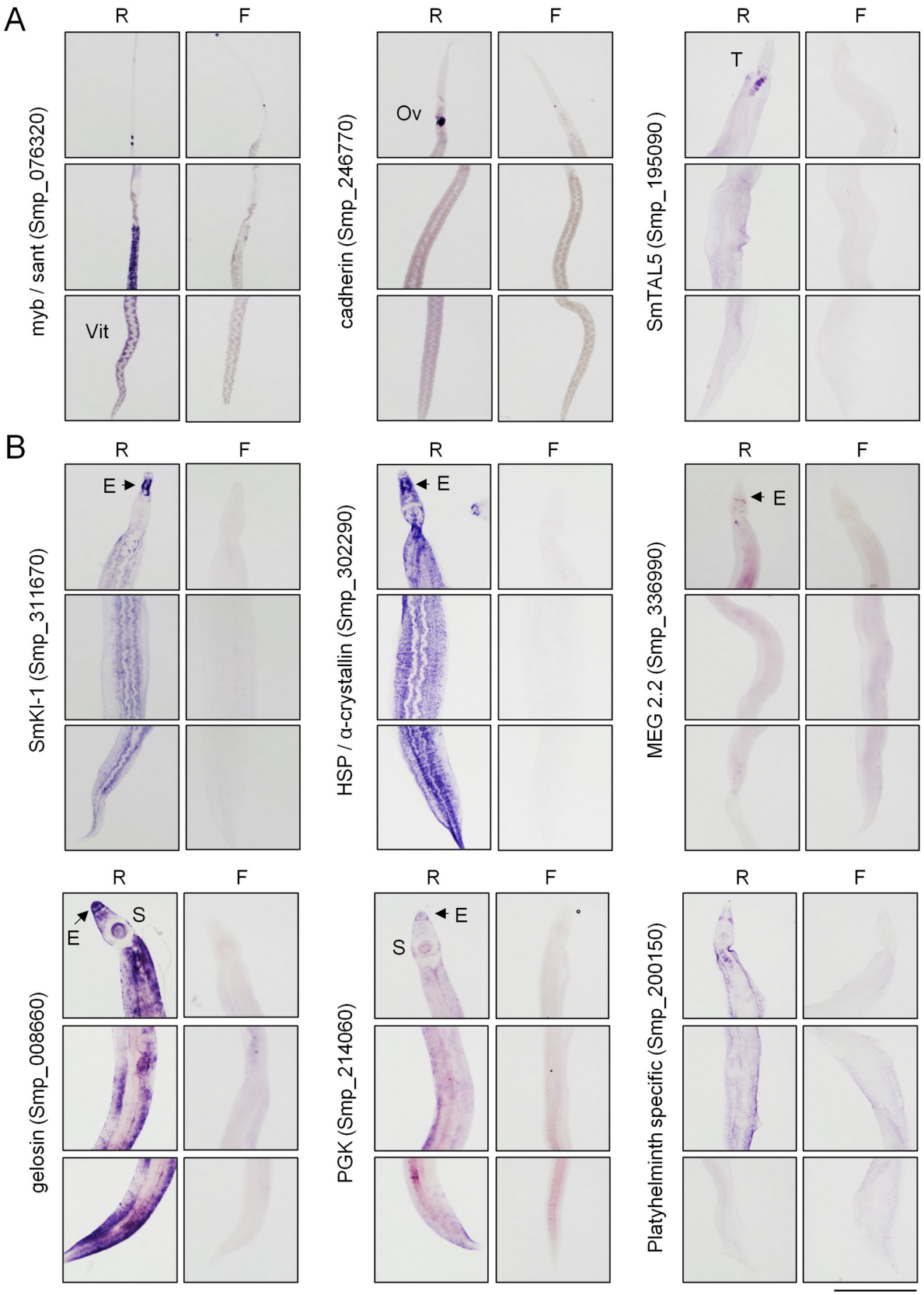
A
R
F
myb / sant (Smp_076320)
Vit
cadherin (Smp_246770)
Ov
SmTAL5 (Smp_195090)
T
B
SmKI-1 (Smp_311670)
E
HSP / α-crystallin (Smp_302290)
E
MEG 2.2 (Smp_336990)
E
gelosin (Smp_008660)
E
S
PGK (Smp_214060)
E
S
Platyhelminth specific (Smp_200150)

Fig 4. Expression patterns of transcripts differentially regulated with praziquantel treatment. *In situ* hybridization of transcripts **(A)** down-regulated and **(B)** up-regulated following *in vivo* PZQ treatment relative to vehicle controls. F = sense negative control probes. R = antisense probes. Images show, from top to bottom, anterior to posterior panels of worms. Ov = ovaries, T = testis, Vit = vitellaria, E = esophagus, S = oral sucker. Scale = 1mm.

https://doi.org/10.1371/journal.pntd.0009200.g004

[27,28]) and occur after the parasite hepatic shift (Fig 1B). They may reflect the parasite response to the change of location within the host, as worms shift from the mesenteric vasculature to the Th2 environment of the granulomatous liver rich in macrophages and granulocytes (Fig 5B).

Discussion

While PZQ has been the frontline anthelmintic used to control schistosomiasis for over 40 years, the drug's molecular mechanism of action is poorly understood. From *in vitro* studies it

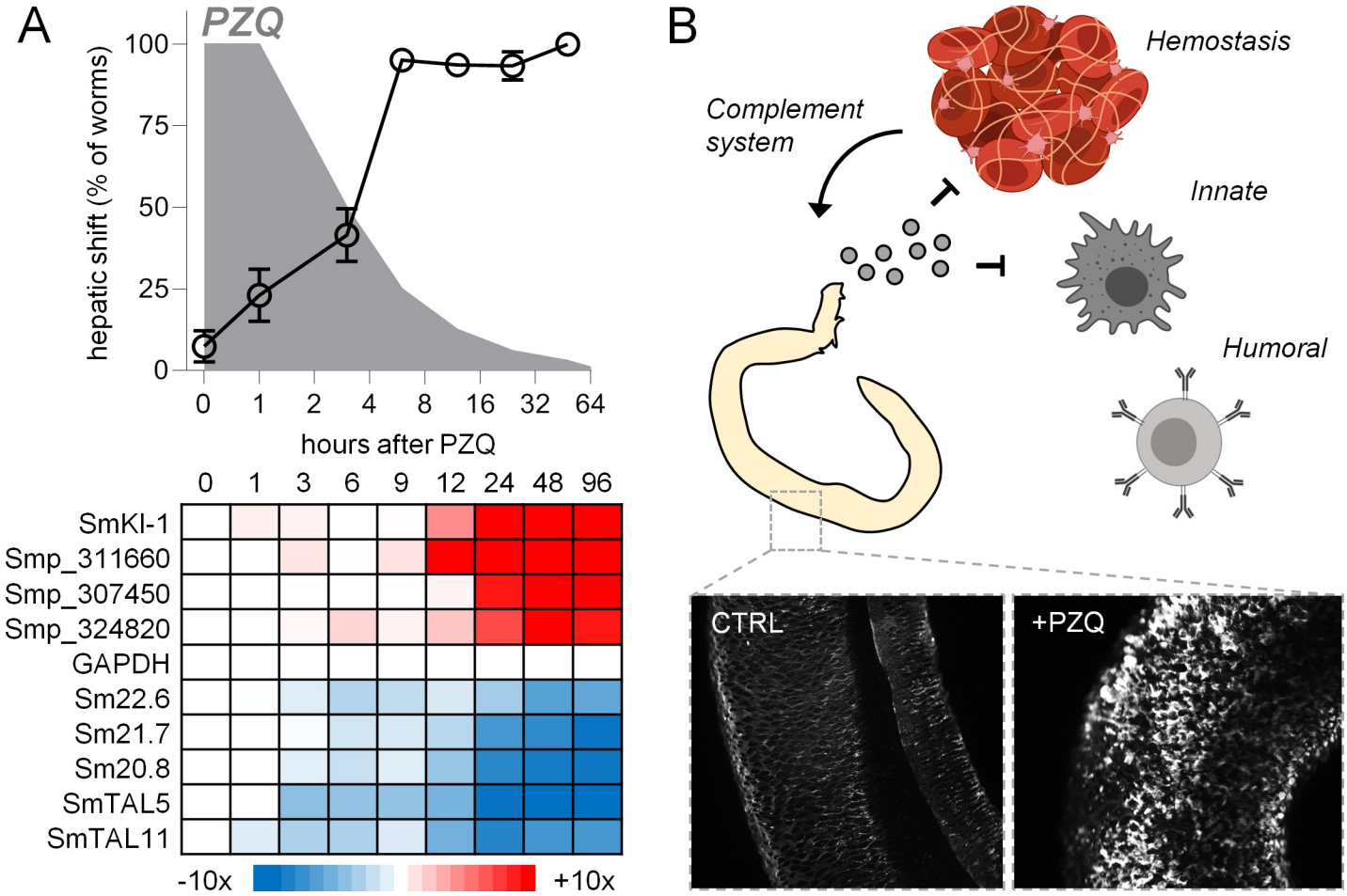

Fig 5. PZQ-evoked changes in immunomodulatory gene products corresponds to the onset of the parasite hepatic shift. (A) *Top*—Kinetics of parasite hepatic shift following PZQ (open symbols, data from Fig 1B) and predicted PZQ elimination in a murine model (grey, data based on refence [28]). *Bottom*—Expression (fold change) of various immunomodulatory gene products such as Kunitz-type protease inhibitors (increasing, red) and tegument-like allergens (decreasing, blue) in worms harvested at various points in the PZQ time-course (data from S1 File). **(B)** Possible model for schistosome release of immunomodulatory signals in response to chemotherapy. Worms normally reside within the host circulatory system, evading detection by the innate and humoral immune system. The parasite tegument is damaged following PZQ exposure, and worms are exposed to the milieu of immune cells within the liver. Secreted signals may dampen the immune response, as well as impair coagulation and resulting activation of the complement pathway. Images created with BioRender.com.

https://doi.org/10.1371/journal.pntd.0009200.g005

is clear that PZQ has pronounced effects on parasite musculature and tegument [5,8]. However, we were interested in several apparent inconsistencies between *in vitro* and *in vivo* observations of PZQ activity. First, it is not clear that PZQ is directly schistocidal *in vivo*. That is, while *in vitro* experiments often measure worm death after periods of drug incubation, PZQ has a short half-life *in vivo* (~2 hours in humans, reviewed in [27], and as short as 30 minutes in mice [28]). Worms harvested from mice after treatment with PZQ indeed display rapid changes in muscle structure within minutes of drug administration (Fig 1D), but this effect was transient. Outcomes such as parasite tegument damage, broad transcriptional changes and death did not occur until hours later—reaching a maximum at one day after drug treatment. Second, PZQ does not cure immature 4-week-old infections [39,40]. This is a clinically important feature of PZQ that may underpin treatment failure in areas of high transmission [41]. However, it is not entirely accurate to say that immature worms are unresponsive to PZQ, since the drug causes contractile paralysis of both 4-week and 7-week-old parasites *in vitro* with approximately equal potency ([8], Fig 3B). Therefore, in order to better understand the effect of *in vivo* PZQ exposure on *S. mansoni*, we performed comparative RNA-Seq on mature and immature worms harvested from PZQ-treated mice. These data provide an overview of not just direct PZQ-evoked changes in gene expression (as may be the case with *in vitro* PZQ treatment [18]), but also the worm response to enviornmental change (i.e. shift from the mesenteric vasucalture to the liver and actions of the host immune system). These gene expression data build upon prior transcriptomic studies [18,19,30,42] and highlight changes in schistosome biology that occur within hours to days after drug treatment, complementing our growing knowledge of PZQ's acute action on parasite targets, such as ion channels that drive Ca^{2+} influx and muscle contraction [6,7], as well as host receptors, such as serotonergic GPCRs that control vasoconstriction [26].

Comparative responses of immature and mature schistosomes to PZQ

The transcriptional response to *in vivo* PZQ exposure is similar between 4-week-old and 7-week-old parasites (Fig 3 and S1 Table)–although mature parasites show greater changes in gene expression, perhaps reflecting a greater sensitivity to chemotherapy. It has been speculated that lack of *in vivo* PZQ efficacy against 4-week-old parasites may be due to PZQ pharmacokinetics, since mature worms within the mesenteric vasculature are exposed to higher drug concentrations prior to first pass metabolism [27,29]. Another possibility is the difference in the host immune environment at the 4-week stage of infection relative to mature infections. In mouse studies, PZQ is less effective against low intensity infections and single sex male infections, which do not lay eggs [43]. The host immune-response to eggs laid by sexually mature worms (i.e. after the ~4 week liver stage juveniles) may contribute to PZQ efficacy. Large numbers of these eggs are deposited in the liver, which results in the recruitment circulating monocytes to the liver and accumulation of alternatively activated macrophages [44]. This hostile immune environment within the livers of mice harboring sexually mature parasites, but not juvenile 4 week old worms, may contribute to the stage-specificity of drug action.

Indeed, differences in both pharmacokinetics and the host immune response may contribute to a lack of PZQ efficacy against juvenile worms. However, it appears that while PZQ causes contractile paralysis (Fig 3B) and tegumental blebbing [8] in both juvenile and adult worms, the neoblast-like cells of immature and mature worms are affected differently by *in vitro* PZQ exposure (Fig 3C). Adult worms show a loss of mitotic activity following PZQ exposure, but juvenile worms are refractory despite the fact that the period of *in vitro* drug incubation used in these assays (14 hours) was far longer than the likely half-life of PZQ *in vivo* (~30 minutes, [28]). One possibility is that there are inherent differences between these stages–

immature worms may harbor more abundant stem cells, such as transitory somatic ε-cells [45]. This may account for treatment failure during these developmental stages.

PZQ causes changes in mRNA levels of putative immunomodulatory gene products

Many of the gene products differentially regulated by PZQ treatment encode proteins that prior studies have implicated in modulation of the host immune system or as putative vaccine targets. For example, the tegument-like allergens (TALs) have been implicated in the host immune-response to infection [37], modulation of clotting [36], and the immune-dependent actions of chemotherapy [46]. Praziquantel has also been shown to interact with several isoforms of recombinant SmTAL (SmTAL 1, 4 & 8) at concentrations in the hundreds of micromolar [47].

A caveat of this study is that transcriptomics data only reflects mRNA levels (changes do not necessarily equate to a readout of protein abundance). However, if transcriptional changes are broadly mirrored by changes in protein levels, then what might be the biological effect of PZQ regulation of immunomodulatory gene products? One possible hypothesis is that worms alter expression of immunomodulatory molecules *in vivo*. Various blood-dwelling parasitic helminths secrete immunomodulatory vesicles into the host circulation [3,48,49], and under normal infection conditions schistosomes modulate components of the host circulatory system. For example, blood from mice harboring patent schistosome infections displays altered clotting properties relative to uninfected mice or mice with immature infections [50]. Parasites may up-regulate anti-clotting signals as an immune-evasion mechanism, since fibrin clots serve as a scaffold for adhesion of granulocytes and monocytes, and activated platelets regulate recruitment and actions of innate immune cells (reviewed in [51]). Schistosomes are susceptible to attack by the host complement system (reviewed in [52]), which is activated by enzymes in the coagulation cascade such as FXa. Therefore, up-regulation of anti-coagulant gene products may enable schistosomes to survive transient PZQ exposure *in vivo* and resume patent infections within the mesenteric vasculature.

Many immunomodulatory gene products are expressed in the schistosome esophagus [38]. These gene products are proposed to protect the parasite from ingested immune components and enzymes found in leukocytes and erythrocytes [33,53]. The schistosome esophagus is also a secretory organ, and it has been speculated that these secretions play a role in parasite immune-evasion [54–57]. PZQ-evoked up-regulation of esophageal transcripts (ex. SmKI-1, HSP) may reflect a schistosome response to evade the host immune recognition triggered either by drug-evoked tegument damage or the hostile immune environment of the liver.

For example, the most enriched group of up-regulated transcripts were Kunitz-type protease inhibitors. One of these, SmKI-1, has been characterized and shown to inhibit neutrophil function [20] and impair blood coagulation via inhibition of enzymes such as Fxa [58]. *In situ* hybridization localized PZQ up-regulated Kunitz-type protease inhibitors to the schistosome esophagus (Fig 4B). Blood-feeding animals harbor various Kunitz-type protease inhibitors with anti-coagulant activity [59] and these proteins are enriched in the salivary proteomes of these organisms [60,61]. Kunitz-type protease inhibitors have also been found in the secretomes of other parasitic flatworms [62,63], and shown to act as ion channel blockers [64] and inhibitors of dendritic cell activation [65]. Additionally, laboratory strains of *S. mansoni* selected for PZQ resistance show altered expression of a various Kunitz-type protease inhibitors, indicating these may be involved in drug resistance [42].

Numerous gene products in the PZQ up-regulated dataset have also been proposed as schistosomiasis vaccine targets. This includes SmKI-1 [66,67], but also cathepsins [68], MEGs [69]

and tetraspanins [70]. Therefore, secreted signals may also promote the development of host antibodies against parasite antigens. Acquired immunity may not be deleterious to existing schistosomes, which are able to survive within the circulatory system alongside host antibodies and immune cells [71], but recognition of parasite antigens may confer immunity to new infections following chemotherapy [72–74].

These data are the first comparative RNA-Seq dataset on *S. mansoni* exposed to PZQ *in vivo*. Our findings confirm changes in gene expression reported in prior *in vitro* studies and microarray experiments, as well as revealing changes in the expression of immunomodulatory gene products that localize to the parasite esophageal glands. Given that several of these gene products, such as the Kunitz-type protease inhibitors, have anti-coagulant effects in both schistosomes and other blood feeding parasites and vectors, these changes may reflect a mechanism employed by schistosomes to actively subvert the hemostatic system and evade the host immune system in response to chemotherapy. These mechanisms inform our basic understanding of parasite interaction with their hosts and provide insight into potential mechanisms for PZQ treatment failure or routes to anthelmintic drug resistance.

Supporting information

S1 Fig. Parasite-specific gene products are differentially expressed in praziquantel treated worms. X-axis = Gene products evidenced by read mapping >0 ranked from most up-regulated to most down-regulated following PZQ treatment. Y-axis = number of transcripts that lack a GO term annotation (top), PFAM protein domain (middle) or BLASTp hit verses the landmark database (bottom) for every 100 gene products.
(TIF)

S2 Fig. Principal component analysis of adult and juvenile parasite transcriptional response to PZQ treatment. Principal component analysis was performed on RNA-Seq data from worms harvested after PZQ 100mg/kg treatment (Figs 2 and 3 and S2 and S3 Files). Blue symbols = control worms, red symbols = PZQ exposed worms. Open symbols = juvenile 4 week infections. Solid symbols = adult 7 week infections.
(TIFF)

S3 Fig. qPCR measurement of PZQ-evoked changes in gene expression. qPCR measurement of select schistosome transcripts identified as differentially expressed by RNA-Seq following PZQ treatment. Up-regulated transcripts = Smp_311670, Smp_324820, Smp_337730, Smp_311630, Smp_340060. Down-regulated transcripts = Smp_086480, Smp_086530, Smp_195090, Smp_169200, Smp_089200, Smp_050270, Smp_013540. Gene expression was measured using worm samples harvested at indicated time points (0–48 hours) following PZQ (400 mg/kg) treatment of mice harboring 7 week old infections. Individual biological replicates are plotted (each consisting of pooled parasites from n = 3 mice per time point), with the averaged data for the three replicates plotted in bold.
(TIFF)

S1 Table. GO-term enrichment in differentially expressed transcripts following PZQ treatment. GO-term enrichment list from up-regulated and down-regulated transcripts (at least two-fold change, FDR adjusted p value < 0.05) for both immature (4-week) and mature (7-week) infections. N.s. = not significant.
(DOCX)

S1 File. Time course RNA-Seq data following *in vivo* PZQ treatment. (Sheet 1) Read counts or **(Sheet 2)** Transcripts Per Million (TPM) for transcripts in worms harvested from mice

treated with PZQ (400mg/kg). **(Sheet 3)** Z-scores of 1848 transcripts with an average TPM >3 and >1 $\log_2$ fold change relative to the t = 0 timepoint that were used to generate the heat map in Fig 1C.
(XLSX)

S2 File. RNA-Seq data for 7-week worms following *in vivo* PZQ treatment. (Sheet 1) Read counts or **(Sheet 2)** Transcripts Per Million (TPM) for transcripts in worms harvested from mice (n = 5) treated with either vehicle control or PZQ (100mg/kg) 7-weeks post-infection. **(Sheet 3)** List of filtered PZQ up and down-regulated transcripts.
(XLSX)

S3 File. RNA-Seq data for 4-week worms following *in vivo* PZQ treatment. (Sheet 1) Read counts or **(Sheet 2)** Transcripts Per Million (TPM) for transcripts in worms harvested from mice (n = 5) treated with either vehicle control or PZQ (100mg/kg) 4-weeks post-infection. **(Sheet 3)** List of filtered PZQ up and down-regulated transcripts.
(XLSX)

S4 File. Primers used in generation of *in situ* hybridization probes. Primer sequences for forward and reverse *in situ* hybridization probes used in Fig 4.
(XLSX)

S5 File. Primers used for qPCR validation of RNA-Seq data. Forward and reverse primer sequences for qPCR measurement of gene expression shown in S3 Fig.
(XLSX)

Acknowledgments

The following reagent was provided by the NIAID Schistosomiasis Resource Center for distribution through BEI Resources, NIH-NIAID Contract HHSN272201700014I. NIH: *Schistosoma mansoni*, Strain NMRI, Exposed Swiss Webster Mice, NR-21963.

Author Contributions

Conceptualization: Paul McCusker, John D. Chan.

Data curation: Paul McCusker, Claudia M. Rohr, John D. Chan.

Formal analysis: Paul McCusker, Claudia M. Rohr, John D. Chan.

Funding acquisition: John D. Chan.

Investigation: Paul McCusker, Claudia M. Rohr, John D. Chan.

Methodology: Paul McCusker.

Project administration: John D. Chan.

Supervision: John D. Chan.

Writing – original draft: John D. Chan.

Writing – review & editing: Paul McCusker, Claudia M. Rohr, John D. Chan.

References

1. van Die I, Cummings RD. Glycan gimmickry by parasitic helminths: a strategy for modulating the host immune response? Glycobiology. 2010; 20(1):2–12. Epub 2009/09/15. https://doi.org/10.1093/glycob/cwp140 PMID: 19748975.

2. Wu C, Hou N, Piao X, Liu S, Cai P, Xiao Y, et al. Non-immune immunoglobulins shield Schistosoma japonicum from host immunorecognition. Sci Rep. 2015; 5:13434. https://doi.org/10.1038/srep13434 PMID: 26299686; PubMed Central PMCID: PMC4547136.
3. Meningher T, Barsheshet Y, Ofir-Birin Y, Gold D, Brant B, Dekel E, et al. Schistosomal extracellular vesicle-enclosed miRNAs modulate host T helper cell differentiation. EMBO Rep. 2019:e47882. Epub 2019/12/12. https://doi.org/10.15252/embr.201947882 PMID: 31825165.
4. Colley DG, Bustinduy AL, Secor WE, King CH. Human schistosomiasis. Lancet. 2014; 383 (9936):2253–64. Epub 2014/04/05. https://doi.org/10.1016/S0140-6736(13)61949-2 PMID: 24698483; PubMed Central PMCID: PMC4672382.
5. Pax R, Bennett JL, Fetterer R. A benzodiazepine derivative and praziquantel: effects on musculature of *Schistosoma mansoni* and *Schistosoma japonicum*. Archives Pharmacol. 1978; 304:309–15. https://doi.org/10.1007/BF00507974 PMID: 714190
6. Kohn AB, Anderson PAV, Roberts-Misterly JM, Greenberg RM. Schistosome calcium channel beta subunits. Unusual modulatory effects and potential role in the action of the antischistosomal drug praziquantel. J Biol Chem. 2001; 40:36873–6. https://doi.org/10.1074/jbc.C100273200 PMID: 11500482
7. Park SK, Gunaratne GS, Chulkov EG, Moehring F, McCusker P, Dosa PI, et al. The anthelmintic drug praziquantel activates a schistosome transient receptor potential channel. J Biol Chem. 2019; 294 (49):18873–80. Epub 2019/10/28. https://doi.org/10.1074/jbc.AC119.011093 PMID: 31653697.
8. Xiao SH, Catto BA, Webster LT Jr., Effects of praziquantel on different developmental stages of Schistosoma mansoni in vitro and in vivo. J Infect Dis 1985; 151(6):1130–7. Epub 1985/06/01. https://doi.org/10.1093/infdis/151.6.1130 PMID: 3998507.
9. Bricker CS, Pax RA, Bennett JL. Microelectrode studies of the tegument and sub-tegumental compartments of male Schistosoma mansoni: anatomical location of sources of electrical potentials. Parasitology 1982; 85 (Pt 1):149–61. Epub 1982/08/01. https://doi.org/10.1017/s0031182000054226 PMID: 7122122.
10. Bricker CS, Depenbusch JW, Bennett JL, Thompson DP. The Relationship between Tegumental Disruption and Muscle-Contraction in *Schistosoma mansoni* Exposed to Various Compounds. Zeitschrift Fur Parasitenkunde-Parasitology Research. 1983; 69(1):61–71. ISI:A1983QC59200007. https://doi.org/10.1007/BF00934011 PMID: 6837102
11. Reimers N, Homann A, Hoschler B, Langhans K, Wilson RA, Pierrot C, et al. Drug-induced exposure of Schistosoma mansoni antigens SmCD59a and SmKK7. PLoS Negl Trop Dis. 2015; 9(3):e0003593. Epub 2015/03/17. https://doi.org/10.1371/journal.pntd.0003593 PMID: 25774883; PubMed Central PMCID: PMC4361651.
12. Panic G, Ruf MT, Keiser J. Immunohistochemical Investigations of Treatment with Ro 13–3978, Praziquantel, Oxamniquine, and Mefloquine in Schistosoma mansoni-Infected Mice. Antimicrob Agents Chemother. 2017; 61(12). Epub 2017/10/04. https://doi.org/10.1128/AAC.01142-17 PMID: 28971860; PubMed Central PMCID: PMC5700362.
13. Sabah AA, Fletcher C, Webbe G, Doenhoff MJ. Schistosoma mansoni: reduced efficacy of chemotherapy in infected T-cell-deprived mice. Exp Parasitol 1985; 60(3):348–54. Epub 1985/12/01. https://doi.org/10.1016/0014-4894(85)90041-4 PMID: 3935473.
14. Brindley PJ, Sher A. The chemotherapeutic effect of praziquantel against Schistosoma mansoni is dependent on host antibody response. J Immunol 1987; 139(1):215–20. PMID: 3108397.
15. Nascimento M, Huang SC, Smith A, Everts B, Lam W, Bassity E, et al. Ly6Chi monocyte recruitment is responsible for Th2 associated host-protective macrophage accumulation in liver inflammation due to schistosomiasis. PLoS pathogens. 2014; 10(8):e1004282. Epub 2014/08/22. https://doi.org/10.1371/journal.ppat.1004282 PMID: 25144366; PubMed Central PMCID: PMC4140849.
16. Barron L, Wynn TA. Macrophage activation governs schistosomiasis-induced inflammation and fibrosis. Eur J Immunol. 2011; 41(9):2509–14. Epub 2011/09/29. https://doi.org/10.1002/eji.201141869 PMID: 21952807; PubMed Central PMCID: PMC3408543.
17. Gönnert R, Praziquantel PA. a new broad-spectrum antischistosomal agent. Z Parasitenkd. 1977; 52 (2):129–50. https://doi.org/10.1007/BF00389899 PMID: 410178
18. Hines-Kay J, Cupit PM, Sanchez MC, Rosenberg GH, Hanelt B, Cunningham C. Transcriptional analysis of *Schistosoma mansoni* treated with praziquantel *in vitro*. Mol Biochem Parasitol. 2012. Epub 2012/10/02. https://doi.org/10.1016/j.molbiopara.2012.09.006 PMID: 23022771.
19. You H, McManus DP, Hu W, Smout MJ, Brindley PJ, Gobert GN. Transcriptional responses of in vivo praziquantel exposure in schistosomes identifies a functional role for calcium signalling pathway member CamKII. PLoS Pathog 2013; 9(3):e1003254. Epub 2013/04/05. https://doi.org/10.1371/journal.ppat.1003254 PMID: 23555262; PubMed Central PMCID: PMC3610926.
20. Morais SB, Figueiredo BC, Assis NRG, Alvarenga DM, de Magalhaes MTQ, Ferreira RS, et al. Schistosoma mansoni SmKI-1 serine protease inhibitor binds to elastase and impairs neutrophil function and

inflammation. PLoS pathogens. 2018; 14(2):e1006870. Epub 2018/02/10. https://doi.org/10.1371/journal.ppat.1006870 PMID: 29425229; PubMed Central PMCID: PMC5823468.

21. Reimand J, Arak T, Adler P, Kolberg L, Reisberg S, Peterson H, et al. g:Profiler-a web server for functional interpretation of gene lists (2016 update). Nucleic Acids Res. 2016; 44(W1):W83–9. Epub 2016/04/22. https://doi.org/10.1093/nar/gkw199 PMID: 27098042; PubMed Central PMCID: PMC4987867.
22. Gerst R, Holzer M. PCAGO: An interactive tool to analyze RNA-Seq data with principal component analysis. bioRxiv. 2019;Preprint number 433078. Epub November 10, 2019. https://doi.org/10.1101/433078
23. King RS, Newmark PA. In situ hybridization protocol for enhanced detection of gene expression in the planarian Schmidtea mediterranea. BMC Dev Biol 2013; 13:8. https://doi.org/10.1186/1471-213X-13-8 PMID: 23497040; PubMed Central PMCID: PMC3610298.
24. Mehlhorn H, Becker B, Andrews P, Thomas H, Frenkel JK. In vivo and in vitro experiments on the effects of praziquantel on Schistosoma mansoni. A light and electron microscopic study. Arzneimittelforschung 1981; 31(3a):544–54. PMID: 7195245.
25. Andrews P. A summary of the efficacy of praziquantel against schistosomes in animal experiments and notes on its mode of action. Arzneimittelforschung 1981; 31(3a):538–41. Epub 1981/01/01. PMID: 7016122.
26. Chan JD, Cupit PM, Gunaratne GS, McCorvy JD, Yang Y, Stoltz K, et al. The anthelmintic praziquantel is a human serotoninergic G-protein-coupled receptor ligand. Nature communications. 2017; 8(1):1910. Epub 2017/12/07. https://doi.org/10.1038/s41467-017-02084-0 PMID: 29208933; PubMed Central PMCID: PMC5716991.
27. Olliaro P, Delgado-Romero P, Keiser J. The little we know about the pharmacokinetics and pharmacodynamics of praziquantel (racemate and R-enantiomer). J Antimicrob Chemother 2014; 69(4):863–70. https://doi.org/10.1093/jac/dkt491 PMID: 24390933.
28. Andrews P. Praziquantel: mechanisms of anti-schistosomal activity. Pharmacol Ther 1985; 29(1):129–56. Epub 1985/01/01. https://doi.org/10.1016/0163-7258(85)90020-8 PMID: 3914644.
29. Abla N, Keiser J, Vargas M, Reimers N, Haas H, Spangenberg T. Evaluation of the pharmacokinetic-pharmacodynamic relationship of praziquantel in the Schistosoma mansoni mouse model. PLoS Negl Trop Dis. 2017; 11(9):e0005942. Epub 2017/09/22. https://doi.org/10.1371/journal.pntd.0005942 PMID: 28934207; PubMed Central PMCID: PMC5626502.
30. Sanchez MC, Krasnec KV, Parra AS, von Cabanlong C, Gobert GN, Umylny B, et al. Effect of praziquantel on the differential expression of mouse hepatic genes and parasite ATP binding cassette transporter gene family members during Schistosoma mansoni infection. PLoS Negl Trop Dis. 2017; 11(6):e0005691. Epub 2017/06/27. https://doi.org/10.1371/journal.pntd.0005691 PMID: 28650976; PubMed Central PMCID: PMC5501684.
31. Fitzpatrick JM, Hirai Y, Hirai H, Hoffmann KF. Schistosome egg production is dependent upon the activities of two developmentally regulated tyrosinases. FASEB J 2007; 21(3):823–35. Epub 2006/12/15. https://doi.org/10.1096/fj.06-7314com PMID: 17167065.
32. Williams DL, Sayed AA, Bernier J, Birkeland SR, Cipriano MJ, Papa AR, et al. Profiling Schistosoma mansoni development using serial analysis of gene expression (SAGE). Exp Parasitol. 2007; 117(3):246–58. Epub 2007/06/20. https://doi.org/10.1016/j.exppara.2007.05.001 PMID: 17577588; PubMed Central PMCID: PMC2121609.
33. Wilson RA, Li XH, MacDonald S, Neves LX, Vitoriano-Souza J, Leite LC, et al. The Schistosome Esophagus Is a 'Hotspot' for Microexon and Lysosomal Hydrolase Gene Expression: Implications for Blood Processing. PLoS Negl Trop Dis. 2015; 9(12):e0004272. Epub 2015/12/08. https://doi.org/10.1371/journal.pntd.0004272 PMID: 26642053; PubMed Central PMCID: PMC4671649.
34. Chalmers IW, Fitzsimmons CM, Brown M, Pierrot C, Jones FM, Wawrzyniak JM, et al. Human IgG1 Responses to Surface Localised Schistosoma mansoni Ly6 Family Members Drop following Praziquantel Treatment. PLoS Negl Trop Dis. 2015; 9(7):e0003920. Epub 2015/07/07. https://doi.org/10.1371/journal.pntd.0003920 PMID: 26147973; PubMed Central PMCID: PMC4492491.
35. Chalmers IW, McArdle AJ, Coulson RM, Wagner MA, Schmid R, Hirai H, et al. Developmentally regulated expression, alternative splicing and distinct sub-groupings in members of the Schistosoma mansoni venom allergen-like (SmVAL) gene family. BMC genomics. 2008; 9:89. Epub 2008/02/26. https://doi.org/10.1186/1471-2164-9-89 PMID: 18294395; PubMed Central PMCID: PMC2270263.
36. Lin YL, He S. Sm22.6 antigen is an inhibitor to human thrombin. Mol Biochem Parasitol 2006; 147(1):95–100. Epub 2006/02/28. https://doi.org/10.1016/j.molbiopara.2006.01.012 PMID: 16499980.
37. Fitzsimmons CM, Jones FM, Stearn A, Chalmers IW, Hoffmann KF, Wawrzyniak J, et al. The Schistosoma mansoni tegumental-allergen-like (TAL) protein family: influence of developmental expression on human IgE responses. PLoS Negl Trop Dis. 2012; 6(4):e1593. Epub 2012/04/18. https://doi.org/10.1371/journal.pntd.0001593 PMID: 22509417; PubMed Central PMCID: PMC3317908.

38. Li XH, Stark M, Vance GM, Cao JP, Wilson RA. The anterior esophageal region of Schistosoma japonicum is a secretory organ. Parasit Vectors. 2014; 7:565. Epub 2014/12/11. https://doi.org/10.1186/s13071-014-0565-8 PMID: 25490864; PubMed Central PMCID: PMC4269844.

39. Sabah AA, Fletcher C, Webbe G, Doenhoff MJ. *Schistosoma mansoni*: chemotherapy of infections of different ages. Exp Parasitol 1986; 61(3):294–303. https://doi.org/10.1016/0014-4894(86)90184-0 PMID: 3086114.

40. Shaw MK. Schistosoma mansoni: stage-dependent damage after *in vivo* treatment with praziquantel. Parasitology 1990; 100 Pt 1:65–72. Epub 1990/02/01. https://doi.org/10.1017/s0031182000060121 PMID: 2107508.

41. Gryseels B, Mbaye A, De Vlas SJ, Stelma FF, Guisse F, Van Lieshout L, et al. Are poor responses to praziquantel for the treatment of Schistosoma mansoni infections in Senegal due to resistance? An overview of the evidence. Trop Med Int Health. 2001; 6(11):864–73. Epub 2001/11/13. https://doi.org/10.1046/j.1365-3156.2001.00811.x PMID: 11703840.

42. Sanchez MC, Cupit PM, Bu L, Cunningham C. Transcriptomic analysis of reduced sensitivity to praziquantel in Schistosoma mansoni. Mol Biochem Parasitol. 2019; 228:6–15. Epub 2019/01/19. https://doi.org/10.1016/j.molbiopara.2018.12.005 PMID: 30658180; PubMed Central PMCID: PMC6372308.

43. Doenhoff MJ, Sabah AA, Fletcher C, Webbe G, Bain J. Evidence for an immune-dependent action of praziquantel on *Schistosoma mansoni* in mice. Trans R Soc Trop Med Hyg 1987; 81(6):947–51. Epub 1987/01/01. https://doi.org/10.1016/0035-9203(87)90360-9 PMID: 3140436.

44. Girgis NM, Gundra UM, Ward LN, Cabrera M, Frevert U, Loke P. Ly6C(high) monocytes become alternatively activated macrophages in schistosome granulomas with help from CD4+ cells. PLoS pathogens. 2014; 10(6):e1004080. Epub 2014/06/27. https://doi.org/10.1371/journal.ppat.1004080 PMID: 24967715; PubMed Central PMCID: PMC4072804.

45. Wang B, Lee J, Li P, Saberi A, Yang H, Liu C, et al. Stem cell heterogeneity drives the parasitic life cycle of Schistosoma mansoni. eLife. 2018; 7. Epub 2018/07/11. https://doi.org/10.7554/eLife.35449 PMID: 29988015; PubMed Central PMCID: PMC6039179.

46. Zhang Z, Xu H, Gan W, Zeng S, Hu X. Schistosoma japonicum calcium-binding tegumental protein SjTP22.4 immunization confers praziquantel schistosomulumicide and antifecundity effect in mice. Vaccine 2012; 30(34):5141–50. Epub 2012/06/12. https://doi.org/10.1016/j.vaccine.2012.05.056 PMID: 22683520.

47. Carson J, Thomas CM, McGinty A, Takata G, Timson DJ. The tegumental allergen-like proteins of Schistosoma mansoni: A biochemical study of SmTAL4-TAL13. Mol Biochem Parasitol 2018; 221:14–22. Epub 2018/02/18. https://doi.org/10.1016/j.molbiopara.2018.02.002 PMID: 29453993.

48. Zamanian M, Fraser LM, Agbedanu PN, Harischandra H, Moorhead AR, Day TA, et al. Release of Small RNA-containing Exosome-like Vesicles from the Human Filarial Parasite Brugia malayi. PLoS Negl Trop Dis. 2015; 9(9):e0004069. https://doi.org/10.1371/journal.pntd.0004069 PMID: 26401956; PubMed Central PMCID: PMC4581865.

49. Samoil V, Dagenais M, Ganapathy V, Aldridge J, Glebov A, Jardim A, et al. Vesicle-based secretion in schistosomes: Analysis of protein and microRNA (miRNA) content of exosome-like vesicles derived from Schistosoma mansoni. Sci Rep. 2018; 8(1):3286. Epub 2018/02/21. https://doi.org/10.1038/s41598-018-21587-4 PMID: 29459722; PubMed Central PMCID: PMC5818524.

50. Da'dara AA, de Laforcade AM, Skelly PJ. The impact of schistosomes and schistosomiasis on murine blood coagulation and fibrinolysis as determined by thromboelastography (TEG). J Thromb Thrombolysis. 2016; 41(4):671–7. Epub 2015/11/18. https://doi.org/10.1007/s11239-015-1298-z PMID: 26573180; PubMed Central PMCID: PMC5467217.

51. Gaertner F, Massberg S. Blood coagulation in immunothrombosis-At the frontline of intravascular immunity. Semin Immunol 2016; 28(6):561–9. Epub 2016/11/22. https://doi.org/10.1016/j.smim.2016.10.010 PMID: 27866916.

52. Skelly PJ. Intravascular schistosomes and complement. Trends Parasitol 2004; 20(8):370–4. Epub 2004/07/13. https://doi.org/10.1016/j.pt.2004.05.007 PMID: 15246320.

53. Li XH, de Castro-Borges W, Parker-Manuel S, Vance GM, Demarco R, Neves LX, et al. The schistosome oesophageal gland: initiator of blood processing. PLoS Negl Trop Dis. 2013; 7(7):e2337. Epub 2013/08/13. https://doi.org/10.1371/journal.pntd.0002337 PMID: 23936568; PubMed Central PMCID: PMC3723592.

54. Felizatti AP, Zeraik AE, Basso LGM, Kumagai PS, Lopes JLS, Wallace BA, et al. Interactions of amphipathic alpha-helical MEG proteins from Schistosomamansoni with membranes. Biochim Biophys Acta Biomembr. 2019:183173. Epub 2019/12/31. https://doi.org/10.1016/j.bbamem.2019.183173 PMID: 31883997.

55. Orcia D, Zeraik AE, Lopes JLS, Macedo JNA, Santos CRD, Oliveira KC, et al. Interaction of an esophageal MEG protein from schistosomes with a human S100 protein involved in inflammatory response.

Biochim Biophys Acta Gen Subj. 2017; 1861(1 Pt A):3490–7. Epub 2016/09/19. https://doi.org/10.1016/j.bbagen.2016.09.015 PMID: 27639541.

56. Neves LX, Wilson RA, Brownridge P, Harman VM, Holman SW, Beynon RJ, et al. Quantitative Proteomics of Enriched Esophageal and Gut Tissues from the Human Blood Fluke Schistosoma mansoni Pinpoints Secreted Proteins for Vaccine Development. Journal of proteome research. 2019. Epub 2019/11/16. https://doi.org/10.1021/acs.jproteome.9b00531 PMID: 31729880.

57. Lee J, Chong T, Newmark PA. The esophageal gland mediates host immune evasion by the human parasite Schistosoma mansoni. Proc Natl Acad Sci U S A. 2020; 117(32):19299–309. Epub 2020/08/02. https://doi.org/10.1073/pnas.2006553117 PMID: 32737161; PubMed Central PMCID: PMC7431036.

58. Ranasinghe SL, Fischer K, Gobert GN, McManus DP. Functional expression of a novel Kunitz type protease inhibitor from the human blood fluke Schistosoma mansoni. Parasit Vectors. 2015; 8:408. Epub 2015/08/05. https://doi.org/10.1186/s13071-015-1022-z PMID: 26238343; PubMed Central PMCID: PMC4524284.

59. Koh CY, Kini RM. Anticoagulants from hematophagous animals. Expert Rev Hematol 2008; 1(2):135–9. Epub 2008/12/01. https://doi.org/10.1586/17474086.1.2.135 PMID: 21082917.

60. Ribeiro JM, Alarcon-Chaidez F, Francischetti IM, Mans BJ, Mather TN, Valenzuela JG, et al. An annotated catalog of salivary gland transcripts from Ixodes scapularis ticks. Insect Biochem Mol Biol. 2006; 36(2):111–29. Epub 2006/01/25. https://doi.org/10.1016/j.ibmb.2005.11.005 PMID: 16431279.

61. Tsujimoto H, Kotsyfakis M, Francischetti IM, Eum JH, Strand MR, Champagne DE. Simukunin from the salivary glands of the black fly Simulium vittatum inhibits enzymes that regulate clotting and inflammatory responses. PLoS One. 2012; 7(2):e29964. Epub 2012/03/03. https://doi.org/10.1371/journal.pone.0029964 PMID: 22383955; PubMed Central PMCID: PMC3285612.

62. Cwiklinski K, de la Torre-Escudero E, Trelis M, Bernal D, Dufresne PJ, Brennan GP, et al. The Extracellular Vesicles of the Helminth Pathogen, Fasciola hepatica: Biogenesis Pathways and Cargo Molecules Involved in Parasite Pathogenesis. Molecular & cellular proteomics: MCP. 2015; 14(12):3258–73. Epub 2015/10/22. https://doi.org/10.1074/mcp.M115.053934 PMID: 26486420; PubMed Central PMCID: PMC4762619.

63. Wang S, Wang S, Luo Y, Xiao L, Luo X, Gao S, et al. Comparative genomics reveals adaptive evolution of Asian tapeworm in switching to a new intermediate host. Nature communications. 2016; 7:12845. Epub 2016/09/23. https://doi.org/10.1038/ncomms12845 PMID: 27653464; PubMed Central PMCID: PMC5036155.

64. Flo M, Margenat M, Pellizza L, Grana M, Duran R, Baez A, et al. Functional diversity of secreted cestode Kunitz proteins: Inhibition of serine peptidases and blockade of cation channels. PLoS pathogens. 2017; 13(2):e1006169. Epub 2017/02/14. https://doi.org/10.1371/journal.ppat.1006169 PMID: 28192542; PubMed Central PMCID: PMC5325619.

65. Falcon CR, Masih D, Gatti G, Sanchez MC, Motran CC, Cervi L. Fasciola hepatica Kunitz type molecule decreases dendritic cell activation and their ability to induce inflammatory responses. PLoS One. 2014; 9(12):e114505. Epub 2014/12/09. https://doi.org/10.1371/journal.pone.0114505 PMID: 25486609; PubMed Central PMCID: PMC4259355.

66. Ranasinghe SL, Duke M, Harvie M, McManus DP. Kunitz-type protease inhibitor as a vaccine candidate against schistosomiasis mansoni. Int J Infect Dis 2018; 66:26–32. Epub 2017/11/13. https://doi.org/10.1016/j.ijid.2017.10.024 PMID: 29128645.

67. Hernandez-Goenaga J, Lopez-Aban J, Protasio AV, Vicente Santiago B, Del Olmo E, Vanegas M, et al. Peptides Derived of Kunitz-Type Serine Protease Inhibitor as Potential Vaccine Against Experimental Schistosomiasis. Front Immunol. 2019; 10:2498. Epub 2019/11/19. https://doi.org/10.3389/fimmu.2019.02498 PMID: 31736947; PubMed Central PMCID: PMC6838133.

68. Hassan AS, Zelt NH, Perera DJ, Ndao M, Ward BJ. Vaccination against the digestive enzyme Cathepsin B using a YS1646 Salmonella enterica Typhimurium vector provides almost complete protection against Schistosoma mansoni challenge in a mouse model. PLoS Negl Trop Dis 2019; 13(12):e0007490. Epub 2019/12/04. https://doi.org/10.1371/journal.pntd.0007490 PMID: 31790394.

69. Martins VP, Morais SB, Pinheiro CS, Assis NR, Figueiredo BC, Ricci ND, et al. Sm10.3, a member of the micro-exon gene 4 (MEG-4) family, induces erythrocyte agglutination in vitro and partially protects vaccinated mice against Schistosoma mansoni infection. PLoS Negl Trop Dis. 2014; 8(3):e2750. Epub 2014/03/22. https://doi.org/10.1371/journal.pntd.0002750 PMID: 24651069; PubMed Central PMCID: PMC3961193.

70. Tran MH, Pearson MS, Bethony JM, Smyth DJ, Jones MK, Duke M, et al. Tetraspanins on the surface of Schistosoma mansoni are protective antigens against schistosomiasis. Nat Med. 2006; 12(7):835–40. Epub 2006/06/20. https://doi.org/10.1038/nm1430 PMID: 16783371.

71. Smithers SR, Terry RJ. Immunity in schistosomiasis. Ann N Y Acad Sci 1969; 160(2):826–40. Epub 1969/10/06. https://doi.org/10.1111/j.1749-6632.1969.tb15904.x PMID: 4981050.

72. Pearson MS, Becker L, Driguez P, Young ND, Gaze S, Mendes T, et al. Of monkeys and men: immunomic profiling of sera from humans and non-human primates resistant to schistosomiasis reveals novel potential vaccine candidates. Front Immunol. 2015; 6:213. Epub 2015/05/23. https://doi.org/10.3389/fimmu.2015.00213 PMID: 25999951; PubMed Central PMCID: PMC4419842.

73. Driguez P, Li Y, Gaze S, Pearson MS, Nakajima R, Trieu A, et al. Antibody Signatures Reflect Different Disease Pathologies in Patients With Schistosomiasis Due to Schistosoma japonicum. J Infect Dis. 2016; 213(1):122–30. Epub 2015/07/08. https://doi.org/10.1093/infdis/jiv356 PMID: 26150545.

74. Gaze S, Driguez P, Pearson MS, Mendes T, Doolan DL, Trieu A, et al. An immunomics approach to schistosome antigen discovery: antibody signatures of naturally resistant and chronically infected individuals from endemic areas. PLoS pathogens. 2014; 10(3):e1004033. Epub 2014/03/29. https://doi.org/10.1371/journal.ppat.1004033 PMID: 24675823; PubMed Central PMCID: PMC3968167.